Proceedings of the Sixth International Conference on
Railway Technology: Research, Development and Maintenance
Edited by: J. Pombo
Civil-Comp Conferences, Volume 7, Paper 9.9
Civil-Comp Press, Edinburgh, United Kingdom, 2024
ISSN: 2753-3239, doi: 10.4203/ccc.7.9.9

Procedure for Wheel-Flat Identification on Railway Wheelset Based on Field and Laboratory Experimental Tests

A. Cavallo[1], M. Bahgat[1], G. Tomasini[1], F. Castelli-Dezza[1], S. Cervello[2] and D. Regazzi[2]

[1] Department of Mechanical Engineering, Politecnico di Milano, Italy
[2] Lucchini RS, Lovere, Italy

Abstract

Detecting wheelset defects early is crucial for maintaining railway safety. Monitoring the condition of wheelsets provides ongoing insights into the system's health, thereby averting the need for time-consuming and costly periodic inspections. This study focuses on identifying wheel-flat defects in railway wheelsets using vibration signals obtained from axle-box measurements. Experimental campaigns were conducted on a wheelset test bench with defects artificially created. These tests aimed to carry out a time domain analysis on the vibration signals and detect features that can highlight the presence and the severity of a wheelset wheel-flat. Subsequently, an experimental campaign through the employment of sensor nodes was carried out on a Mercitalia freight train (Car T3000) to validate the obtained results.

Keywords: railway wheelset, wheel-flat, axle-box, vibration measurements, in line, laboratory experimental tests, sensor node, condition monitoring.

1 Introduction

The need for detecting and preventing failures in high-risk industries, such as the railway one, becomes essential to support the system's operational efficiency and, of course, human safety. Maintenance, particularly predictive maintenance, plays a vital role in ensuring railway safety by minimizing failures and costs without compromising productivity [1]. Unlike Corrective and Preventive maintenance, Predictive maintenance needs direct monitoring of the mechanical conditions to process real-time data and predict possible signs of failure. Instead of relying on routine checks based on failure models, predictive maintenance schedules tasks as they become necessary based on equipment condition [2, 3]. Leveraging the Industrial Internet of Things, which continuously assesses machinery states, offers a proactive, data-driven approach [4] to identifying problems. This approach helps mitigate risks and eliminates the need for costly, time-sensitive interventions.

Addressing wheelset defects is crucial in railway condition monitoring discussions, given their potential to cause severe disturbances and possibly failures. Monitoring of railway vehicles can happen through sensors installed on the railway infrastructure, e.g. *Wayside Monitoring* [5], or through sensors placed on the vehicle itself, e.g. *On-board Monitoring* [6]. Exhaustive research, both academic and commercial, is being carried out focusing on the topic of on-board condition monitoring, as it allows to rely on algorithms properly tuned for the specific vehicle and can perform continuous analysis. In [7], different approaches to on-board wheel condition monitoring are investigated, including magnetic, ultrasonic and acoustic techniques. Vibrational detection techniques are also available, some of them concerning the employment of axle-boxes acceleration, i.e. ABA, signals: the latter can indeed be considered quite reliable as they gather vibrational data very close to the possible source of the problem ([8, 9]).

The focus of this work is the identification by means of on-board ABA measurements of a specific wheelset defect, *Wheel-flat*. Wheel-flat is a wheel geometry profile defect caused by wheel locking during the breaking process and successive sliding on the rail. It is one of the most common local surface defects and can cause further degradation of wheels, bearings suspensions and track with time. The identification of said defect can be achieved in many ways ([10, 11]), but often by ABA vibration measurements. Indeed, the presence of a wheel-flat induces in the vertical acceleration a peak value at every complete rotation of the wheel in correspondence of the angle of rotation for which the wheel-flat is passing through the contact point between wheel and rail. Liang et al. [12] developed a simplified mathematical model and a simulation of the wheel-flat and rail surface defects, which were later compared with experimental results from force and acceleration signals, ABA ones included, of a roller rig. Time domain features such as Crest Factor, Skewness, RMS and peak values were tested, coupled with time-frequency techniques as Short Time Fourier Transform, Wigner-Ville transform and Wavelet Transform. In [13], Bai et al. present a wheel-flat diagnosis method based on frequency-domain Gramian angular field of

ABA signals, investigating the frequency domain rather than the time domain.

Most of the existing algorithms for wheel-flat defect identification require a synchronous sample of the acceleration signal, obtained by means of a direct measure of vehicle speed. This can be obtained with an encoder or from the GPS signal. In [14], Empirical Mode Decomposition, i.e. EMD, was adopted for wheel-flat detection in the railway field, while requiring an approximate estimation of the wheel rotational speed. The issue with this method is that it is costly in terms of computational power, which represents a problem for on-board sensor specifics. Time-domain detection methods are definitely more advantageous. Bosso et al. [15] propose to use ABA measured on vehicles and to analyze it in the time domain to detect wheel-flats. An algorithm was developed based on the measurement of the vertical acceleration and tested on numerical simulations and experimental tests. The drawback is that an encoder is used to determine the angular position of the wheelset and the algorithm is designed to work in a nearly constant speed condition. Furthermore, the algorithm is tested on a Y25 freight train and validated with a maximum speed admissible of $90\,\mathrm{km/h}$ with a sampling frequency of $1\,\mathrm{kHz}$.

This paper aims to define a procedure to detect wheel-flat through key features of ABA signals. The methodology involves extracting time domain features from vibration signals. Experimental tests are conducted on the Lucchini RS BU300 full-scale test bench, followed by trials on an operational railway vehicle. The novelty of this approach lies in its ability to derive wheelset rotational speed directly from acceleration measurements, bypassing the need for an encoder measurement. This is accomplished by implementing the Cepstral Analysis, which is performed by reversing the methodology proposed by Baasch et al. in [16], aimed at the identification of the wheel radius from the previously obtained speed.

2 BU300 Experimental Tests

A set of experimental tests is performed, to investigate the sensitivity of the time domain for the identification of wheel-flat in a real full-scale setting. The experimental tests were conducted on the BU300 roller rig test bench which is located in Lovere (BG) Italy at the industrial facility of Lucchini RS. In this section, the test bench with the measuring set-up is described, along with the tests schedule and the testing procedure adopted.

2.1 Experimental Set-up

A picture of the BU300 test bench can be seen in Figure 1(a), whilst a technical scheme is observable in Figure 1(b). On the rig, a full-scale train wheelset is put in rotation by means of the contact with two disks with a $2\,\mathrm{m}$ diameter having a profile similar to the standard UIC60. The two disks are rigidly connected and driven by a DC motor which allows a maximum peripheral speed of $300\,\mathrm{km/h}$. A set of three

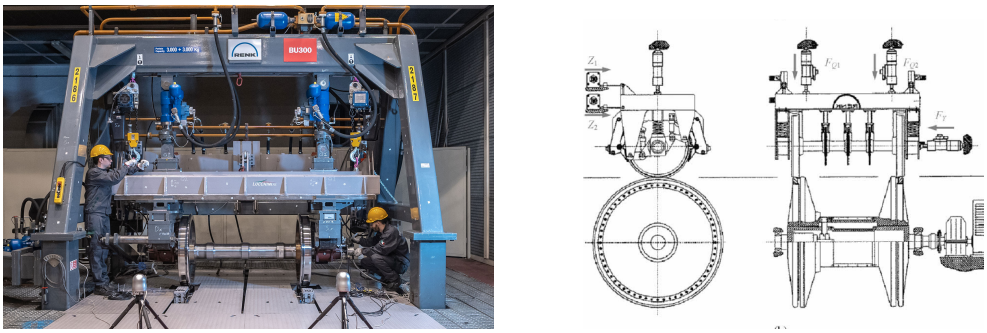

(a) (b)

Figure 1: (a) The Lucchini RS BU300 full-scale roller rig. (b) The BU300 full-scale roller rig scheme from [18].

hydraulic actuators impose the vertical and lateral load and four electro-mechanical actuators are used for the lateral positioning of the wheelset with respect to the rail. The test bench can reproduce multiple conditions, constant speed, acceleration, and braking, both on tangent track and in curve conditions. Further information on the described roller rig and its control system can be found in [17] and in [18]. For the acquisition, two tri-axial piezoelectric cabled accelerometers are placed in the axle-boxes, thus both on the right and on the left of the axle. The accelerometers model is 356A06, with a full-scale of $500\,\mathrm{g}$: the three directions of interest (vertical, longitudinal, lateral) are thus acquired without saturation issues.

2.2 Test Conditions

A set of various experimental campaigns was run in order to gather sets of data in which railway wheelsets were tested in three conditions. In one of them, artificially created defects were reproduced by means of manufacturing processes.

For wheel-flat investigation, five different conditions were tested, which are listed in Table 1. They are identified by the length and the width of the defect. From now on, wheel-flat will be addressed as WF, coupled with a number that identifies its increasing size. The defect was generated starting from the smallest one, WF1, and its dimensions were increased each time after an acquisition cycle. An example of a reproduced wheel-flat can be seen in Figure 2. On the other hand, the label NO DEFECT indicates a set of data sampled with any kind of defect artificially reproduced and without any kilometer run beforehand.

The test modality adopted is the same for each tested condition. The full-scale wheelset at the test bench is put in rotation and the speed is increased up to $100\,\mathrm{km/h}$. When the regime condition is reached, 5 subsequent acquisitions are started. Afterward, the speed is increased up to $200\,\mathrm{km/h}$, and again the sampling is carried out. Eventually, the speed is increased up to $300\,\mathrm{km/h}$, and, after sampling at said speed, the latter is gradually reduced to 0 and the cycle is over.

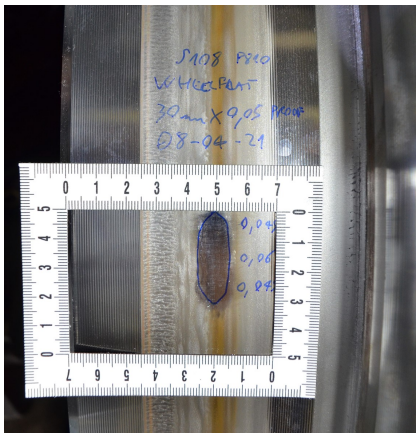

Figure 2: Experimental tests: picture of the reproduced WF3 defect of length $30\,\mathrm{mm}$ and depth about $0.05\,\mathrm{mm}$

As a consequence, for each defect size, three speeds were tested, $100\,\mathrm{km/h}$, $200\,\mathrm{km/h}$ and $300\,\mathrm{km/h}$. The acquisitions for tests labeled WF2. were damaged, therefore their data were discarded.

2.3 Defect Identification Features

2.3.1 Raw Data Analysis

Wheel-flat data are analyzed in time domain, since, as previously stated, the presence of a wheel-flat on the wheel profile generates acceleration peaks in the vertical direction. Figure 3 shows the acquired time histories for WF data, focusing on $1\,\mathrm{s}$ of each signal for each velocity. On the y-axis, there is the vertical direction acceleration. The growing size of the defect corresponds to a significant effect on the vertical acceleration peaks, and this becomes evident by looking at WF1 versusWF5 time histories. Moreover, the last statement can be considered valid, especially for the signals measured at $100\,\mathrm{km/h}$.

Defect Name	**Length** [mm]	**Heigth** [mm]
WF1	10	2e-2
WF2	30	2e-2
WF3	30	5e-2
WF4	30	8e-2
WF5	60	8e-2

Table 1: Experimental tests Wheel-flat defects dimensions definition.

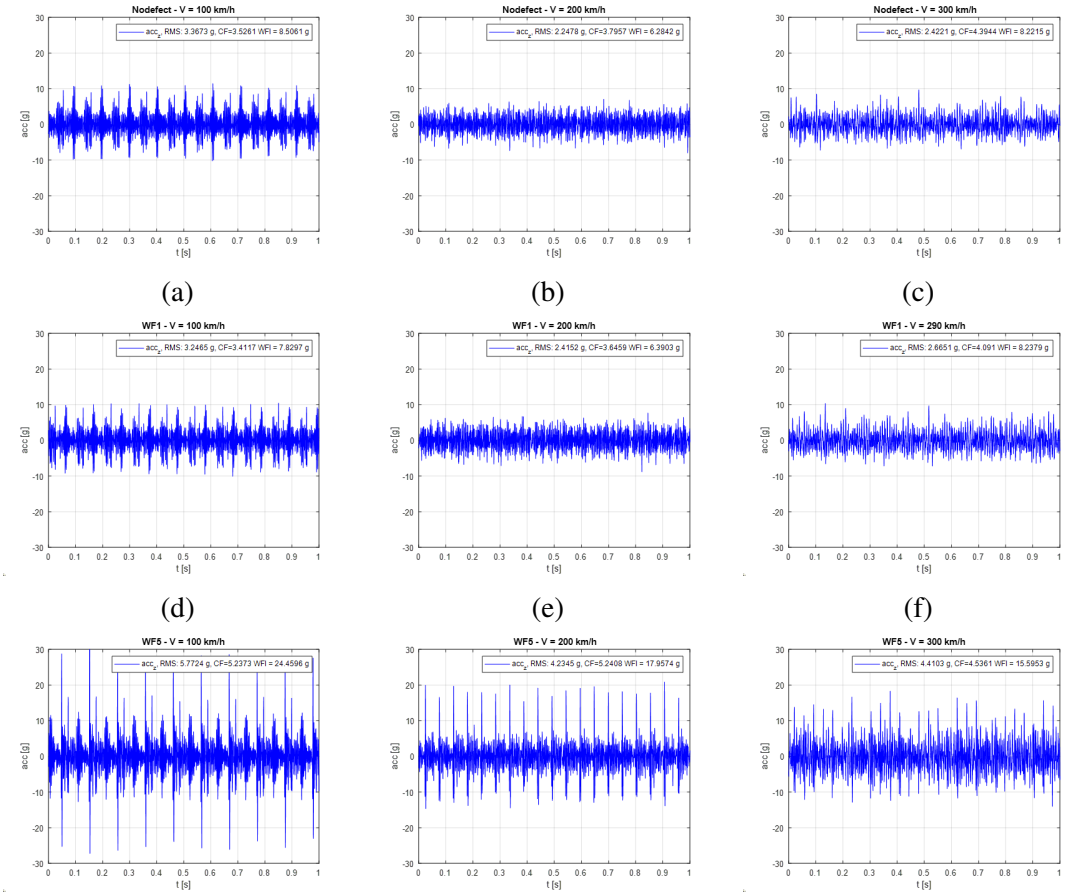

(a) (b) (c)

(d) (e) (f)

(g) (h) (i)

Figure 3: Time Domain Analysis: from NO DEFECT to highest Wheel-Flat WF5 for increasing speeds (low, medium and high). One second time history, vertical acceleration signal.

2.3.2 Features Extraction

Features extraction is carried out on the acquired signals according to the following principle: the acceleration signal contribution related to the presence of the wheel-flat is periodic with the wheel revolution. The latter concept means that all the information on the defect is present in the acceleration signal of a single wheel revolution. In a real case scenario, the same signal contains also components uncorrelated to the presence of the defect, e.g. track irregularities, which need to be filtered out. To do this, the knowledge of the rotational speed allows one to cut the single acquisitions in many sub-windows all correlated to one another. Also, it allows to building a statistically significant dataset as, from one acquisition, a number multiple of the revolution period, called *fundamental* period, is generated.

Each acquisition is cut into windows a fundamental period long. To do this, the wheel rotational velocity is identified by reversing the algorithm presented in Baash et

al.[16]: the algorithm takes as an input the known wheel radius and the acceleration signals and, by computing the cepstrum, it estimates the wheel velocity. The algorithm is run independently on the three measured directions (longitudinal, lateral, vertical) and the results are cross-checked to detect anomalies. The output of the cepstral analysis is considered valid if lying on a $\pm 5\%$ with respect to the nominal speed used on the test bench acquisitions. If the condition is verified, the results are averaged among the directions and the final value is assigned to the fundamental period.

Considering the existing literature works, for each window a fundamental period long, the following time features are computed.

- Root Mean Square, i.e. RMS. It shows the overall mean power of the signal;
- Crest Factor, i.e. CF. It identifies peaks with respect to the RMS. Being an a-dimensional index, it focuses on the identification of the shape of the signal itself regardless of its amplitude.
- Wheel-Flat severity Index, i.e. WFI. This index allows quantifying the presence of peaks in the signal whilst keeping its dependence on the overall amplitude of the signal and peaks. It is a dimensional index defined in [15].

2.4 Results

For each tested speed (see Subsection 2.2) the extracted features are shown in 2-dimensional plots: CF vs RMS and WFI vs RMS. Wheel-flat presence is tested by comparing the signals with absence of defects, i.e. NO DEFECT dataset.

Figures 4(a), 4(b), 4(c) show the 2D features representation CF vs RMS comparing the different levels of wheel-flat with the NO DEFECT condition for each tested speed. In Figure 4(d), 4(e), 4(f) the same signals are shown using the 2D feature plot representation WFI vs RMS.

We can see a significant effect caused by the presence of WF. Both representations are able to catch a significant difference between the NO DEFECT and the most severe wheel-flat level, WF5. WF4 and WF5 data are quite distinguishable, especially in Figure 4(a) and Figure 4(d). In any case, a visual inspection of the plots also highlights how low-speed vertical acceleration signals ($100\,\mathrm{km/h}$) are more suitable for wheel-Flat identification than high-speed ones ($300\,\mathrm{km/h}$).

3 In line Experimental Tests

An experimental campaign is carried out by fixing four sensor nodes on a freight train wagon moving cargo between Verona (Italy), and Hamburg and Cologne (Germany). The sensors were fixed on the axle-boxes of a Y25 bogie.

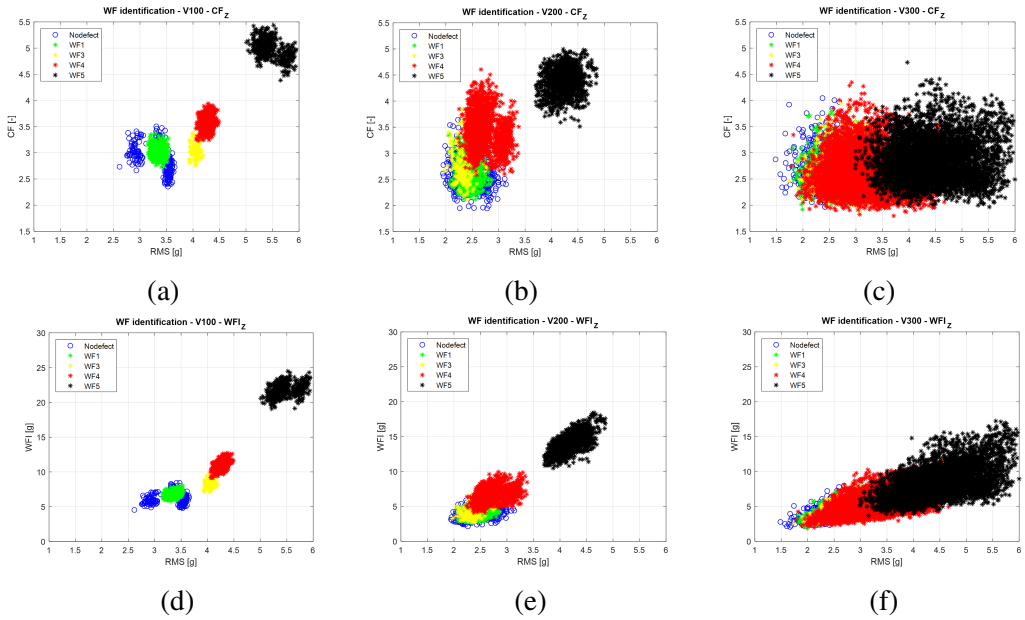

Figure 4: 2D features plot at 100 km/h, 200 km/h, 300 km/h.: CF vs RMS (a, b, c) and WFI vs RMS (d, e, f). In blue the NO DEFECT data, in green WF1, in yellow WF3, in red WF4, in black WF5.

3.1 Set-Up

Four nodes have been named and placed as indicated in Figure 5(a). Two of them were powered by a 12V on-board battery (NODE 2 and NODE 9), recharged by a wheel hub generator. The remaining two (NODE 4 and NODE 6) were equipped with photovoltaic panels, i.e. PV, for harvesting solar energy. The nodes were fixed as shown in Figure 5(b). It is worth adding that NODE 2 and NODE 9 were mounted on a wheelset which had wheels just reprofiled before the start of the campaign.

3.2 Data Sampling

Vibrational signals in the vertical direction were sampled from the four nodes starting on November 17, 2022 and ending on February 2, 2023. The nodes were designed to transmit via GSM every two hours, by capturing the train velocity from a GPS module mounted on each node. The signals were captured by triaxial accelerometers with a sampling frequency of $3.3\,\mathrm{kHz}$. Each signal was $7.8\,\mathrm{s}$ long. As the employed sensors were prototypes, some issues occurred due to battery management, GPS connection (vital for velocity recording) and GSM connection. As a consequence, the totality of gathered acquisitions can be summarised in Table 2.

For the missing data about the train velocity, the Cepstral method was employed (refer to Section 2.3.2). As the BU300 experimental tests were carried out at 100, 200, $300\,\mathrm{km/h}$, considering that that maximum velocity of the freight train was $120\,\mathrm{km/h}$, the velocity within the interval $98 - 102\,\mathrm{km/h}$ were included in this analysis. The

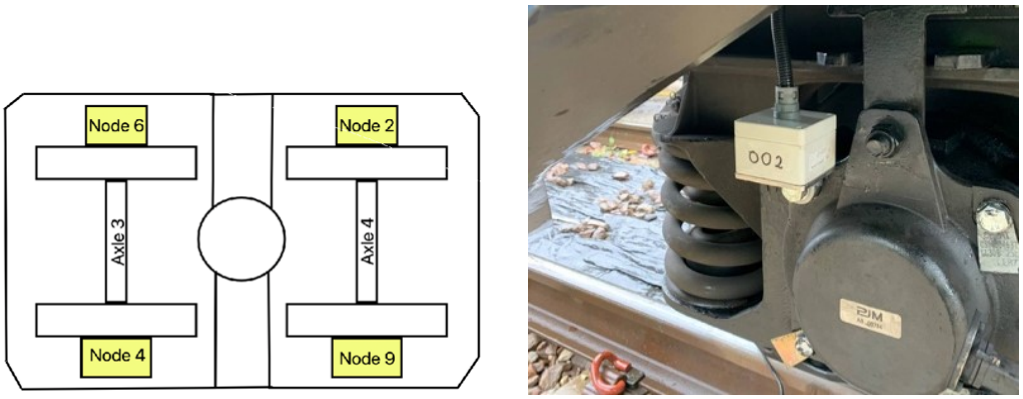

(a) (b)

Figure 5: (a) Setup and location of mounted nodes on the train wagon. (b) Field test: pictures of NODE 2 after mounting.

total considered acquisitions are explained in Table 3.

3.3 Data Analysis

This analysis is carried out with the purpose of capturing differences in the nature of the signal between field experiments representing realistic operating conditions and laboratory experiments held in a controlled environment.

3.3.1 Features Extraction and Results

To present a clear comparison, the same procedures described for the laboratory data were applied to the field database.

For wheel-flat detection, the following time domain features are computed for each signal and for each time window a fundamental period long (see Section 2.3.2): RMS, CF, WFI.

Data processing was carried out with two objectives: to understand the validity of the experimental campaign and to draw a comparison with the experimental data

	Node 2	**Node 9**	**Node 4**	**Node 6**
Total# Acq.	738	2815	111	86
No Velocity recorded	148	531	42	29
Zero Velocity Recorded	514	2155	69	53
Recorded Velocity Above Zero	76	129	0	4

Table 2: Statistics about the recorded speed of the acquisitions in the time period $11.17.22 - 02.16.23$

	Node 2	Node 9	Node 4	Node 6
Velocity Recorded from GPS in the range	8	18	0	0
Correctly detected by Cepstral Analysis (GPS comparison)	8	17	0	0
Detected by Cepstral Analysis (NO GPS comparison)	46	192	17	10
Total extended # Acq.	54	210	17	10

Table 3: Extended field database considering the acquisition with train velocity within $[98, 102]\,\mathrm{km/h}$

gathered with the tests performed at the BU300 test bench.

As *Axle 4* (see Figure 5(a)) had wheel just reprofiled, data related to NODE 2 and NODE 9 are hereby showed. By looking at the simultaneous acquisition of the latter in terms of the mentioned features, the range of features is clustered within the same range for both nodes with some samples outside of this range. It can be concluded that both nodes are performing similarly. The samples outside of the clustering range are mostly from the same signals. This can be related to impulses from external factors that happen in the signal that cause some windows to have higher feature values (Figure 6). Furthermore, even though it was expected to notice an increase in the RMS values over time for increasing wear levels, there was no time trend noticed in the values of the features so far (i.e. values are not increasing or decreasing with time). The total distance covered by the train during the whole campaign is not known but between the 22nd of December and the 14th of February, the train has covered approximately 20,000 km based on given travel records.

Figure 4(a) and Figures 6(a) and 6(b) represent the CF vs RMS plots of laboratory data and field data of the z-axis, sampled at $100\,\mathrm{km/h}$ and $98\,\mathrm{km/h} - 102\,\mathrm{km/h}$, respectively. The following remarks can be highlighted: by observing the plots, we can conclude that the majority of the nodes data lie within RMS$= [0.5, 2]g$, whilst CF$= [2, 5]$. Those ranges are considered out of the ranges achieved by any distinguishable wheel-flat, data which is characterized by having RMS$= [4, 7]g$ and CF$= [3, 7]$. Additionally, the range for those features is lower than ranges of NO DEFECT data, as field data signals being characterized by lower RMS values. The lower RMS for the field signals is related to a rail-wheel contact that is different from the experimental setup. Furthermore, it can be noticed that the field data spread on a range where some of the samples can be classified as Wheel-flat: this phenomenon is due to the stochastic nature of the field signal, where some windows can have high feature values due to field outliers.

On the other hand, Figure 4(d) and Figures 6(c) and 6(d) represent the WFI vs RMS plots of laboratory data and field data of the z-axis, sampled at $100\,\mathrm{km/h}$ and $98\,\mathrm{km/h} - 102\,\mathrm{km/h}$, respectively. For this representation, most of the nodes data

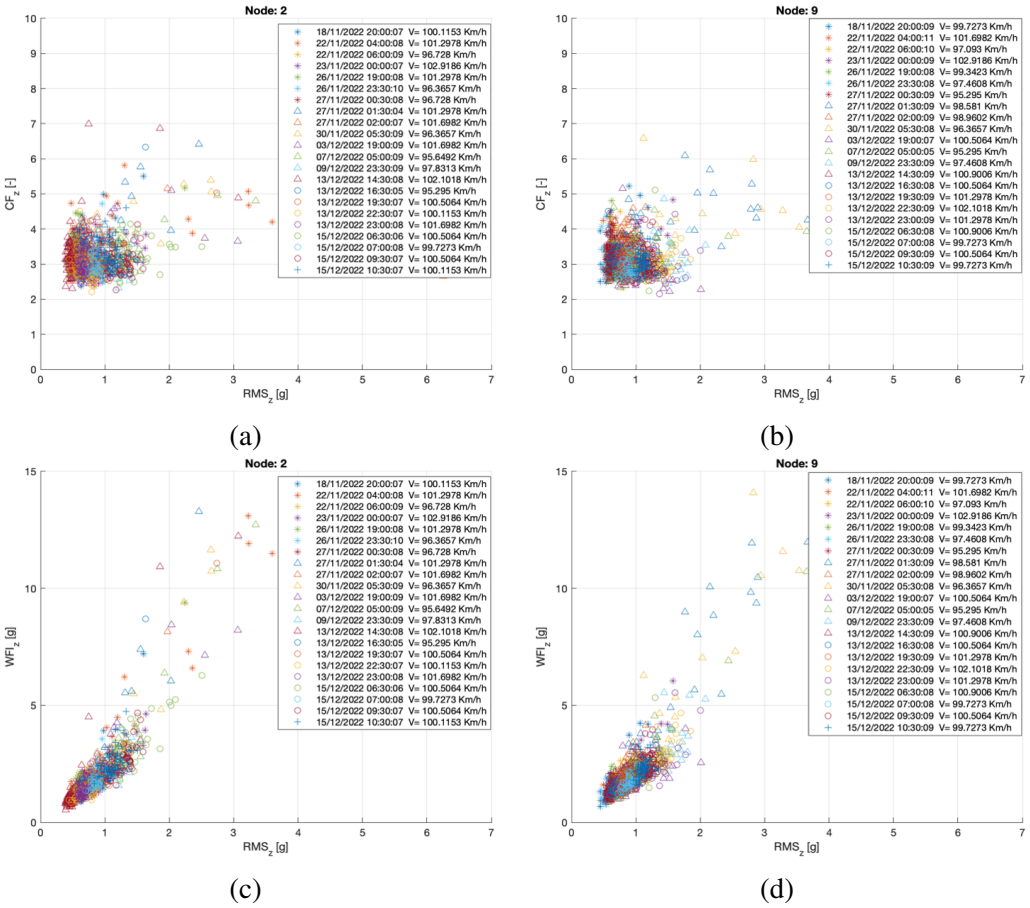

Figure 6: CF vs RMS plot, node 2 (a) and node 9 (b), and WFI vs RMS plot, node 2 (c) and node 9 (d). Each point in the plot represents a window of the signal. All points with the same shape and color are windows from the same signal.

lie within CF$= [0.5, 5]$, which is a range far from any distinguishable wheel-flat data, characterized by having WFI values in the range CF$= [7.5, 27.5]$.

The latest conclusions were expected, considering that the monitored wheelset was checked and reprofiled before being installed. In addition, given standard working conditions, no wheel-flat was expected to arise in such a short time.

4 Conclusions

This paper discusses an investigation into identifying Wheel-flat in railway wheelsets using acceleration measurements obtained from on-board axle-box sensors. Experimental tests on a full-scale wheelset at Lucchini RS BU300 test bench are described, showing data for different wheel conditions at different speeds. The time domain features for the wheel-flat identification are extracted for each window of length equal to the fundamental period, cut from the original acquisition. To do this, the revolu-

tion speed is directly computed from the ABA signals through the *cepstral analysis*, without the aid of any external device. The identification of wheel-flat presence is investigated through 2D plots featuring CF vs RMS and WFI vs RMS. The comparison with NO DEFECT data leads to the conclusion that WF4 and WF5 are easily distinguishable, especially as low speed, i.e. $100\,\mathrm{km/h}$. Afterward, an experimental campaign is carried out on a real-life railway vehicle, where four on-board sensors are installed on two wheelset axle-boxes: the signals captured within three months are then studied to capture the differences with the test-bench data at $100\,\mathrm{km/h}$. For their analysis *cepstral analysis* was employed, allowing the employment of a great sample of data even though GPS velocity was not available. Field data, in terms of CF vs RMS and WFI vs RMS, had values, as expected, out of range of any wheel-flat. The latest observation was expected, due to outliers and different train-track interaction. In addition, it was expected that no defect would occur in the passed time frame.

In subsequent phases, experimental trials will be conducted across various vehicle types to expand the current database and verify the achieved results. Moreover, a series of experimental tests involving artificially induced defects on an in-line vehicle will be imperative to compare the features values in the presence of defects.

References

[1] Narjes Davari, Bruno Veloso, Gustavo de Assis Costa, Pedro Mota Pereira, Rita P. Ribeiro, and João Gama. A survey on data-driven predictive maintenance for the railway industry. *Sensors*, 21(17), 2021.

[2] R Keith Mobley. *An introduction to predictive maintenance*. Elsevier, 2002.

[3] Binder Mario, Vitaliy Mezhuyev, and Martin Tschandl. Predictive maintenance for railway domain: a systematic literature review. *IEEE Engineering Management Review*, 2023.

[4] Qianyi Chen, Jiannong Cao, and Songye Zhu. Data-driven monitoring and predictive maintenance for engineering structures: Technologies, implementation challenges, and future directions. *IEEE Internet of Things Journal*, 2023.

[5] Muhammad Zakir Shaikh, Zeeshan Ahmed, Bhawani Shankar Chowdhry, Enrique Nava Baro, Tanweer Hussain, Muhammad Aslam Uqaili, Sanaullah Mehran, Dileep Kumar, and Ali Akber Shah. State-of-the-art wayside condition monitoring systems for railway wheels: A comprehensive review. *IEEE Access*, 2023.

[6] Esteban Bernal, Maksym Spiryagin, and Colin Cole. Onboard condition monitoring sensors, systems and techniques for freight railway vehicles: a review. *IEEE Sensors Journal*, 19(1):4–24, 2018.

[7] Alireza Alemi, Francesco Corman, and Gabriel Lodewijks. Condition monitoring approaches for the detection of railway wheel defects. *Proceedings of the Institution of Mechanical Engineers, Part F: Journal of Rail and Rapid Transit*, 231(8):961–981, 2017.

[8] Bo Xie, Shiqian Chen, Maoyong Dong, Shunqi Sui, Chao Chang, and Kaiyun Wang. Detection of wheel diameter difference of railway wagon by acmd-fbd and optimized mkelm. *IEEE Transactions on Instrumentation and Measurement*, 71:1–11, 2022.

[9] Qi Sun, Chunjun Chen, Andrew H Kemp, and Peter Brooks. An on-board detection framework for polygon wear of railway wheel based on vibration acceleration of axle-box. *Mechanical Systems and Signal Processing*, 153:107540, 2021.

[10] J Brizuela, C Fritsch, and A Ibáñez. Railway wheel-flat detection and measurement by ultrasound. *Transportation research part C: emerging technologies*, 19(6):975–984, 2011.

[11] Massimo Leonardo Filograno, Pedro Corredera, Miguel Rodriguez-Plaza, Alvaro Andres-Alguacil, and Miguel Gonzalez-Herraez. Wheel flat detection in high-speed railway systems using fiber bragg gratings. *IEEE Sensors journal*, 13(12):4808–4816, 2013.

[12] Bo Liang, SD Iwnicki, Yunshi Zhao, and David Crosbee. Railway wheel-flat and rail surface defect modelling and analysis by time–frequency techniques. *Vehicle System Dynamics*, 51(9):1403–1421, 2013.

[13] Yongliang Bai, Jianwei Yang, Jinhai Wang, and Qiang Li. Intelligent diagnosis for railway wheel flat using frequency-domain gramian angular field and transfer learning network. *Ieee Access*, 8:105118–105126, 2020.

[14] Yifan Li, Jianxin Liu, Yan Wang, et al. Railway wheel flat detection based on improved empirical mode decomposition. *Shock and Vibration*, 2016, 2016.

[15] Nicola Bosso, Antonio Gugliotta, and Nicolò Zampieri. Wheel flat detection algorithm for onboard diagnostic. *Measurement*, 123:193–202, 2018.

[16] Benjamin Baasch, Judith Heusel, Michael Roth, and Thorsten Neumann. Train wheel condition monitoring via cepstral analysis of axle box accelerations. *Applied Sciences*, 11(4):1432, 2021.

[17] S Bruni, F Cheli, and F Resta. A model of an actively controlled roller rig for tests on full-size railway wheelsets. *Proceedings of the Institution of Mechanical Engineers, Part F: Journal of Rail and Rapid Transit*, 215(4):277–288, 2001.

[18] Francesco Braghin, Stefano Bruni, and Giorgio Diana. Experimental and numerical investigation on the derailment of a railway wheelset with solid axle. *Vehicle System Dynamics*, 44(4):305–325, 2006.